Influence of Dispersion Interactions on the Thermal Desorption of Nonplanar Polycyclic Aromatic Hydrocarbons on HOPG

Jürgen Weippert, Philipp Huber, Ayla Schulz, Konstantin Y. Amsharov, Artur Böttcher,* and Manfred M. Kappes

A combination of low energy ion beam deposition and mass resolved thermal desorption spectroscopy is applied to analyze the binding behavior of two nonplanar polycyclic aromatic hydrocarbons (PAHs) to highly oriented pyrolytic graphite (HOPG) surfaces—also concerning their lateral dispersion interactions. In particular, the fullerene precursor $C_{60}H_{30}$ (FPC) and rubrene $C_{42}H_{28}$ are studied. Due to their smaller contact areas, both molecules exhibit significantly weaker binding energies to the HOPG surface compared to planar PAHs of similar size: $C_{60}H_{30}$ is bound to the surface by 3.04 eV, which is 0.6 eV lower than for a fully planar homologue. For rubrene, an isolated molecule–substrate binding energy of 1.59 eV is found, which is about 1 eV less than that of the corresponding planar homologue hexabenzocoronene $C_{42}H_{18}$. In contrast to FPC, rubrene shows a significant (intermolecular) lateral dispersion contribution to the binding energy as the submonolayer coverage increases.

The scaling of physisorption energies with size for homologous series of organic molecules on well-defined surfaces is of increasing interest toward benchmarking theoretical descriptions of

Dr. J. Weippert, P. Huber, A. Schulz, Dr. A. Böttcher, Prof. M. M. Kappes
Institute of Physical Chemistry
KIT
76131 Karlsruhe, Germany
E-mail: artur.boettcher@kit.edu

Dr. J. Weippert
EP-HT Group
Fraunhofer Institute for Applied Solid State Physics
79108 Freiburg, Germany

Dr. K. Y. Amsharov
Institute of Organic Chemistry II
Friedrich-Alexander-Universität Erlangen-Nürnberg
91058 Erlangen, Germany

Prof. M. M. Kappes
Institute of Nanotechnology
KIT
76344 Eggenstein-Leopoldshafen, Germany

ⓘ The ORCID identification number(s) for the author(s) of this article can be found under https://doi.org/10.1002/pssr.201900348.

dispersion interactions (and their dependence on localization and transfer of charge).[1] Recently, we have applied temperature-programmed desorption (TPD) spectroscopy to determine the desorption energies of a range of large flat polycyclic aromatic hydrocarbons (PAHs) on graphite and have used these values to provide a more accurate estimation of the graphite interlayer cohesion energy by extrapolation.[2] We found that the desorption energies were not measurably influenced by lateral interactions between the fully planar PAHs, despite the fact that theoretical calculations[3] predicted a significant contribution of such interactions to the overall binding energies. There were two possible explanations for this observation: either the calculations strongly overestimated the lateral dispersion energy, or the desorption occurs in a two-step mechanism in which an adsorbed molecule first detaches from an island on the surface, diffuses onto a free surface area, and then desorbs from there. If the former is true, this leads to an obvious question: how much does the structure of PAH adsorbates have to deviate from full planarity to observe significant lateral dispersion energy contributions to the desorption energy?

To investigate this, we have applied the same experimental procedures as described in detail in our work on planar PAHs[2] now for two nonplanar species: 1) the fullerene precursor $C_{60}H_{30}$ (FPC; synthesized in the Amsharov group according to literature procedures[4,5]), which has been found to give rise to well-organized arene-stacked multilayers[4,6] due to its three slightly twisted "wings" (**Figure 1**) and 2) rubrene $C_{42}H_{28}$ (Rub, Acros, 99%), which has four phenyl rings standing almost perpendicularly to its central tetracene unit. The molecular structure of rubrene as determined by X-ray diffraction (XRD)[7] shows one of the biggest deviations from planarity that could be imagined for a PAH. The rubrene adsorption geometry on highly oriented pyrolytic graphite (HOPG) has been characterized by scanning tunneling microscopy (STM) measurements:[8,9] the central tetracene unit is oriented practically parallel to the surface.

Both FPC and rubrene were adsorbed onto HOPG (SPI supplies, SPI-2 and TipsNano, ZYB) using the low energy ion beam deposition setup described in our previous study.[2,10] Parent cations were generated by electron impact ionization of the
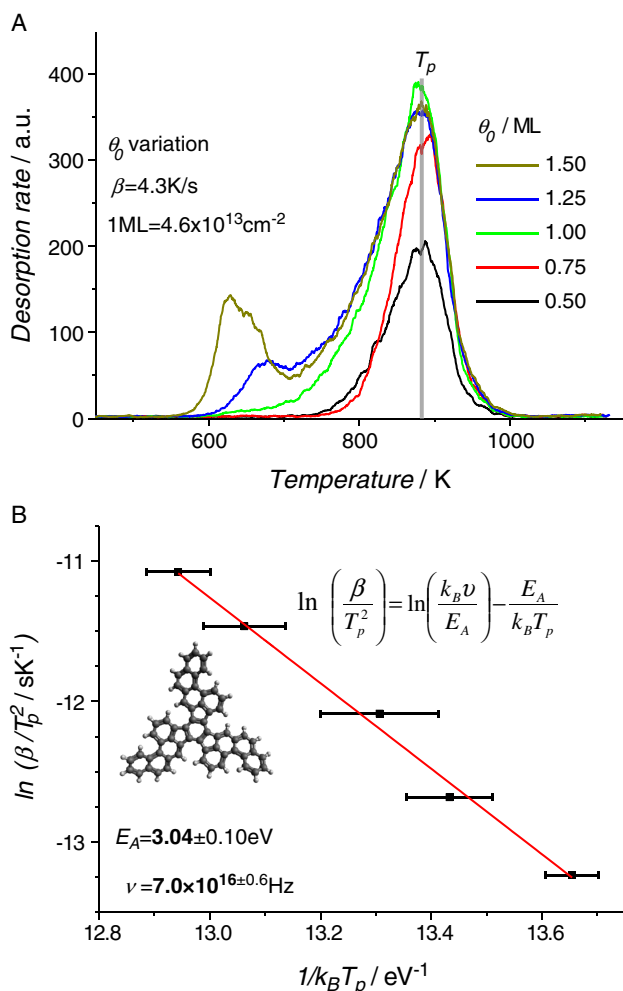
A

B

Figure 1. Thermal desorption of the nonplanar PAH $C_{60}H_{30}$ (FPC) from HOPG. A) Coverage variation series to verify the first-order desorption and to determine the ML equivalent ion dose. B) Heating rate variation plot with an initial coverage of 0.75 ML (full set of spectra in the Supporting Information).

corresponding sublimed neutral species. Selection of the incident ion beam according to mass-to-charge ratio ensured that the resulting film was free of impurities present in the powder samples or of ionization-induced fragments corresponding to acetylene or phenyl loss. Dehydrogenated fragments could not be resolved and may be present in minor amounts, which leads to the formation of dimers that desorb at temperatures above the ranges shown here. After deposition of the desired number of ions, mass-selective TPD was applied in situ as previously described[2] (FHI-ELAB GO74 temperature ramp generator and Extrel Merlin mass spectrometer, Keller PZ-2 pyrometer for surface temperature calibration) to monitor the desorption rates of both species. The TPD spectra acquired in this manner were then analyzed with methods based on the Polanyi–Wigner equation[11]

$$-r_{\mathrm{Des}}(t) = \frac{\mathrm{d}\theta}{\mathrm{d}t} = \nu_n \theta^n \exp\left(-\frac{E_A}{RT}\right) \quad (1)$$

where ν is the frequency factor, n is the reaction order, θ is the coverage, and E_A is the activation energy for the desorption, which is basically equivalent to the binding energy.

For FPC, the results are summarized in Figure 1: by systematically varying the coverage, we were also able to identify the multilayer desorption onset (secondary desorption peak at ≈650 K), from which we determined the monolayer (ML) equivalent coverage to be 4.6×10^{13} ions cm^{-2}. We then see that, for various initial submonolayer coverages, the maximum of the desorption rate is always found at 880 K. This means that the desorption order is one, and that the lateral interactions to other FPC molecules are negligible. It is noteworthy that the multilayer peak edge and maximum shift toward lower temperatures for a higher coverage, whereas, for planar PAHs, the opposite has been found to be the case.[12] It has been established in the literature[13,14] that differences between monolayer and multilayer desorption temperatures may also be influenced by entropic effects. Correspondingly, we interpret the observed downshift for FPC, as indicating that the aforementioned stacked FPC multilayers[4,6] have a lower entropy than stacks of planar PAHs.

As the slight twist of the three "wings" apparently is not enough to result in a measurable lateral dispersion interaction, the desorption of FPC can, therefore, be analyzed with the first-order methods such as for a fully planar PAH. It is likely that the FPC–HOPG interaction may lead to deviations from the shown gas phase structure, but a fully planar adsorption geometry is impossible due to steric hindrance. This, in turn, allows us to use the heating rate variation (HRV) method[15] to determine the binding energy and the frequency factor. In this method, the temperatures T_p at which the desorption reaches its maximum for a given heating rate β is plotted in the following manner:

$$\ln\left(\frac{\beta}{T_p^2}\right) = \ln\left(\frac{k_B \nu}{E_A}\right) - \frac{E_A}{k_B T_p} \quad (2)$$

As shown in Figure 1B, this method results in a binding energy of 3.04 ± 0.10 eV and a frequency factor of $7.0 \times 10^{16 \pm 0.6}$ Hz (for the full set of underlying spectra, please refer to the Supporting Information). It is interesting to compare the FPC number to various other 60 carbon species whose binding energies to HOPG have been measured by TPD—both as a function of molecular structure and hydrogenation degree. **Table 1** summarizes the corresponding desorption parameters of four different species: the fully planar PAHs $C_{60}H_{22}$ (indexed

Table 1. Binding energies and frequency factors for various 60 C-atom species having different types of molecular topology as indicated. "HRV" refers to the heating rate variation method as applied in this work for FPC, whereas "RK" refers to a TPD analysis based on assumed frequency factors with a numerical Runge–Kutta solution of the Polanyi–Wigner equation.

Molecule	Structure	Method	ν (Hz)	E_A (eV)
$C_{60}H_{22}$ (HTC)	Planar	HRV[2]	3.9×10^{18}	3.65
$C_{60}H_{24}$ (TRC)	Planar	HRV[2]	3.1×10^{18}	3.59
$C_{60}H_{30}$ (FPC)	Twisted	HRV	7.0×10^{16}	3.04
C_{60}	Fullerene	RK[16]	$10^{13.2}$	0.85

ADVANCED SCIENCE NEWS
www.advancedsciencenews.com

pss rrl
physica status solidi
www.pss-rapid.com

HTC in ref. [2]) and $C_{60}H_{24}$ (TRC) studied by us previously,[2] the "winged" FPC investigated here and buckminsterfullerene C_{60}.

The "winged" FPC has a binding energy which is 0.5–0.6 eV lower than those of its two planar homologues. This can be rationalized by the fact that not all atoms in the FPC adsorbates can have the same distance to the surface. According to a DFT-calculated structure (Turbomole,[17] RI-B3LYP,[18–22] and def2-TZVP[23]), the highest-positioned, i.e., most "out-of-plane" carbon atoms must have a ca. 1 Å larger distance to the surface. A deeper analysis requires taking structural relaxation effects into account and goes beyond the scope of this study. It is, however, interesting to note that the frequency factor for FPC is two orders of magnitude lower than for the planar 60-atom PAHs. According to previous studies,[3,13,24] a lower frequency factor indicates a more mobile adsorbate species (= high entropy). As the effective contact area between FPC and HOPG is smaller than for a planar PAH homologue, an enhanced mobility seems quite plausible. This effect is even more pronounced for fullerene C_{60}.[16]

For rubrene, the coverage variation experiments (shown in the spectra in **Figure 2**A) show a fundamentally different behavior: the temperature T_p of the desorption rate maxima shifts from 450 K for low coverages up to 480 K for a saturated ML. This means that the almost perpendicular phenyl rings give rise to a measurable lateral binding energy. Interestingly, the multilayer signal sets in at an unusually high ion dose (four times higher than found previously for the planar PAH homologue hexabenzocoronene $C_{42}H_{18}$[2]). This might be an indicator that, for higher submonolayer coverages, the structure of the rubrene film changes similar to what is seen for pentacene where a planar to tilted herringbone packing transition has been discussed.[25–27] For further analysis, we will use $1\,\text{ML} = 1.8 \times 10^{14}\,\text{ions cm}^{-2}$ based on the multilayer signal onset and the termination of the T_p shift. Note that such a film structure change would not affect the primary conclusion, namely, that there is a lateral contribution to the overall binding energy as seen by the systematic upshift of T_p. Therefore, we cannot use the heating rate variation method to determine the binding energy (in the Supporting Information, we show what happens if we do). Instead, we fit the experimental data by comparison with calculated desorption rates derived by the fourth-order Runge–Kutta integration (RK4) of a Polanyi–Wigner equation with a modified activation energy as used, e.g., in the determination of lateral C_{60} interactions[16] or similar studies[28,29]

$$E_A = E_{RS} + z\theta E_{RR} \qquad (3)$$

Here, E_{RS} is the rubrene-substrate binding energy, E_{RR} is the mean lateral rubrene–rubrene binding energy per neighboring molecule, and z is the lateral coordination number. Based on the fact that all previously investigated PAHs[2] have shown the first-order desorption behavior and taking into consideration that the shape of the TPD spectra shown here does not deviate dramatically from these previous PAH studies, we also assume the first-order desorption behavior for rubrene. According to STM investigations[8,9] of rubrene films on graphite, it has six neighbors in a saturated monolayer. It is known that in bulk crystals[9] or on stronger interacting surfaces[30] the twisted tetracene unit gets straightened; it is not fully investigated whether this is
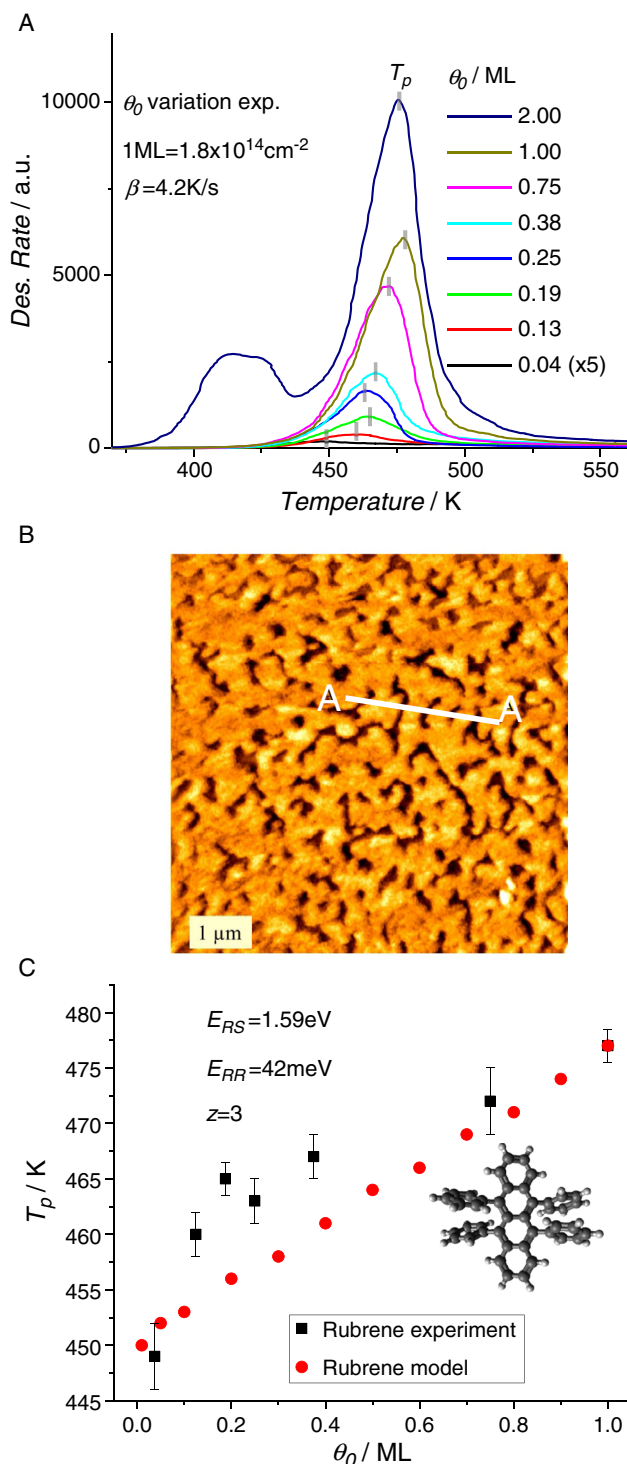
Figure 2. A) TPD coverage variation series for the desorption of rubrene from HOPG at a fixed heating rate of $\beta = 4.2\,\text{Ks}^{-1}$ (lowest coverage scaled up for better visibility) experimental results (tailing at higher temperatures indicates some desorption from defect sites). B) AFM image ($1 \times 1\,\mu\text{m}^2$) for an almost saturated ML of rubrene on HOPG with giraffe-skin pattern as generated by soft landing in this study (a height profile along the marked path can be found in the Supporting Information). C) Comparison of the T_p development in the experimental and simulated coverage variation series.

also the case on HOPG, but it does not affect the outcome of this analysis. Our own AFM measurements (Figure 2B) also suggest that the rubrene islands resulting from soft landing do not grow in a fully isotropic manner, but rather form a "giraffe-skin pattern." Therefore, it would ideally be necessary to take into account several differently oriented neighbors in analyzing the lateral interactions. However, in the absence of additional structural information, we have instead used the simple assumption of "half-shell" ($z = 3$) coordination to simulate a range of TPD spectra for various values of E_{RS} and E_{RR} and for submonolayer coverages ranging from 0.01 up to 1.00.

In the corresponding Runge–Kutta integrations, we have estimated the unknown rubrene frequency factor by assuming that it corresponds to the experimentally determined value for hexabenzocoronene, $2.9 \times 10^{17 \pm 1.3}$ Hz,[2] since it is the only experimentally investigated PAH homologue with an identical number of carbon atoms. The coverage dependence of the peak maximum T_p is best reconstructed using $E_{RS} = 1.59$ eV and $E_{RR} = 42$ meV (corresponding to an overall lateral energy contribution of $3 \times 42 = 126$ meV), as shown in Figure 2C (please refer to the Supporting Information for the full set of simulated spectra as well as a more detailed survey on T_p values). While the simulated $T_p(\theta_0)$ development is almost linear, the experimental values show a nonlinear behavior for a low θ_0. This may be the result of a lower effective coordination at lower coverages, i.e., a stronger deviation from the $z = 3$ approximation.

The E_{RS} value of 1.59 eV can additionally be differentiated into contributions of the tetracene backbone and the phenyl rings in direct contact with the substrate. In our previous work,[2] we had determined increments for the PAH–HOPG dispersion energy based on a theoretical model by Björk et al.[31] For tetracene, at a graphite interlayer distance of 3.4 Å, this leads to a binding energy of 1.29 eV. Our AFM measurements (see Figure 2B and Supporting Information) imply that the tetracene unit should be found at ca. 5 Å from the surface. As molecule–surface interactions scale with the quartic distance,[32] this means that the tetracene backbone contributes ≈ 0.25 eV to the binding energy, leaving each phenyl ring to contribute 0.33 eV.

In closing, it is interesting to put our rubrene measurement into a wider context. As already stated, lateral interactions between flat PAHs on HOPG are negligibly small. By contrast, lateral interactions between alkyl side chains of functionalized PAHs can be strong enough to dominate self-organization of the corresponding films.[33–36] Rubrene–rubrene dispersion interactions contributed to mainly by the phenyl functional groups on their respective tetracene backbones fall somewhere in between. At 42 meV, the mean lateral rubrene–rubrene binding energy is little smaller than that of an isolated benzene dimer, which according to numerous spectroscopic[37–42] and theoretical[43–45] studies has a binding energy of ≈ 100 meV for the energetically favored T-shaped geometry. Also of comparable magnitude are the dispersive interactions on the order of 10 meV per aromatic side group,[46] which contribute to the self-organization of large biomolecules. By contrast, the lateral dispersive interactions in a fullerene ML on HOPG are significantly larger amounting to ≈ 280 eV per C_{60} pair,[16,47] reflecting both larger molecular dimensions and enhanced nonplanarity.
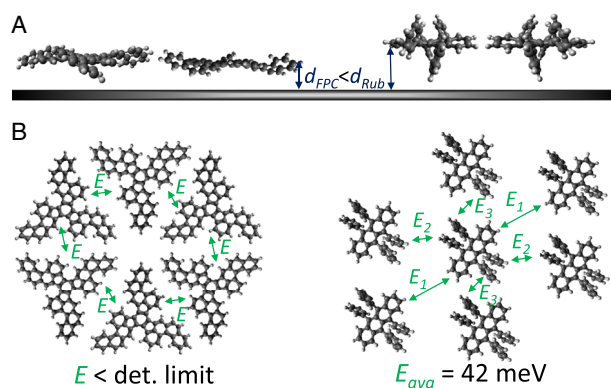

Figure 3. A) Schematic side-on representations of the adsorption geometries of FPC and rubrene on HOPG (structures calculated for isolated molecules): the mean separation of the atoms in FPC from the graphite basal plane (d_{FPC}) is smaller than for most atoms in rubrene (d_{Rub}), which explains the lower molecule–substrate binding energy of the latter. B) While FPC (schematic layer structure is speculative) shows no measurable lateral interaction, rubrene (exact adsorbate structure from STM[8,9]) has a mean lateral binding energy of 42 meV. Based on the rubrene adsorbate structure, binding energies E_2 and E_3 involving closely situated phenyl rings would be expected to contribute more to the average lateral binding energy E_{avg} than E_1, which reflects primarily the interaction between (almost planar) tetracene units.

Figure 3 summarizes our observations. While the only slightly twisted FPC does not extend sufficiently out of plane to yield a measurable lateral interaction, rubrene–rubrene lateral interactions amount to 42 meV.

Supporting Information

Supporting Information is available from the Wiley Online Library or from the author.

Acknowledgements

Conflict of Interest

The authors declare no conflict of interest.

Keywords

ADVANCED SCIENCE NEWS
www.advancedsciencenews.com

pss rrl
physica status solidi
www.pss-rapid.com

[1] F. Maass, M. Ajdari, F. C. Kabeer, M. Vogtland, A. Tkatchenko, P. Tegeder, *J. Phys. Chem. Lett.* **2019**, *10*, 1000.

[2] J. Weippert, J. Hauns, J. Bachmann, A. Böttcher, X. Yao, B. Yang, A. Narita, K. Müllen, M. M. Kappes, *J. Chem. Phys.* **2018**, *149*, 194701.

[3] J. D. Thrower, E. E. Friis, A. L. Skov, L. Nilsson, M. Andersen, L. Ferrighi, B. Jorgensen, S. Baouche, R. Balog, B. Hammer, L. Hornekaer, *J. Phys. Chem. C* **2013**, *117*, 13520.

[4] O. de Frutos, B. Gómez-Lor, T. Granier, M. A. Monge, E. Gutiérrez-Puebla, A. M. Echavarren, *Angew. Chem. Int. Ed.* **1999**, *38*, 204.

[5] M. Kabdulov, M. Jansen, K. Y. Amsharov, *Chem. Eur. J.* **2013**, *19*, 17262.

[6] L. T. Scott, M. M. Boorum, B. J. McMahn, S. Hagen, J. Mack, J. Blank, H. Wegner, A. de Meijere, *Science* **2002**, *295*, 1500.

[7] O. D. Jurchescu, A. Meetsma, T. T. M. Palstra, *Acta Crystallogr. B* **2006**, *62*, 330.

[8] T. Ueba, J. Park, R. Terawaki, Y. Watanabe, T. Yamada, T. Munakata, *Surf. Sci.* **2016**, *649*, 7.

[9] C. Udhardt, R. Forker, M. Gruenewald, Y. Watanabe, T. Yamada, T. Ueba, T. Munakata, T. Fritz, *Thin Solid Films* **2016**, *598*, 271.

[10] A. Böttcher, P. Weis, A. Bihlmeier, M. M. Kappes, *Phys. Chem. Chem. Phys.* **2004**, *6*, 5213.

[11] M. Polanyi, E. Wigner, *Z. Phys. Chem.* **1928**, *139*, 439.

[12] R. Zacharia, H. Ulbricht, T. Hertel, *Phys. Rev. B* **2004**, *69*, 155406.

[13] M. Roos, A. Breitruck, H. E. Hoster, R. J. Behm, *Phys. Chem. Chem. Phys.* **2010**, *12*, 818.

[14] P. Frank, N. Koch, M. Koini, R. Rieger, K. Müllen, R. Resel, A. Winkler, *Chem. Phys. Lett.* **2009**, *473*, 321.

[15] J. Falconer, R. Madix, *Surf. Sci.* **1975**, *48*, 393.

[16] H. Ulbricht, G. Moos, T. Hertel, *Phys. Rev. Lett.* **2003**, *90*, 095501.

[17] TURBOMOLE V7.1 2016, a development of University of Karlsruhe and Forschungszentrum Karlsruhe GmbH, **1989–2007**, (Turbomole GmbH since 2007), available from http://www.turbomole.com.

[18] A. Becke, *J. Chem. Phys.* **1993**, *98*, 5648.

[19] S. Vosko, L. Wilk, M. Nusair, *Can. J. Phys.* **1980**, *58*, 1200.

[20] C. Lee, W. Yang, R. Parr, *Phys. Rev. B* **1988**, *37*, 785.

[21] A. Becke, *Phys. Rev. A* **1988**, *38*, 3098.

[22] K. Eichkorn, F. Weigend, O. Treutler, R. Ahlrichs, *Theor. Chem. Acc.* **1997**, *97*, 119.

[23] F. Weigend, M. Häser, H. Patzelt, R. Ahlrichs, *Chem. Phys. Lett.* **1998**, *294*, 143.

[24] D. Käfer, C. Wöll, G. Witte, *Appl. Phys. A* **2009**, *95*, 273.

[25] M. Klues, G. Witte, *CrystEngComm* **2018**, *20*, 63.

[26] J. Götzen, D. Käfer, C. Wöll, G. Witte, *Phys. Rev. B* **2010**, *81*, 085440.

[27] H. Yang, L. Huang, K. Sun, K. Niu, Z. Cui, H. Zhang, Z. Wang, D. Yan, L. Chi, *J. Phys. Chem. C* **2017**, *121*, 25043.

[28] L. Zommer, L. Sobiński, *Pol. J. Chem.* **1999**, *73*, 339.

[29] L. Sobiński, L. Zommer, *Pol. J. Chem.* **1999**, *73*, 1373.

[30] D. Käfer, G. Witte, *Phys. Chem. Chem. Phys.* **2005**, *7*, 2850.

[31] J. Björk, F. Hanke, C. A. Palma, P. Samori, M. Cecchini, M. Persson, *J. Phys. Chem. Lett.* **2010**, *1*, 3407.

[32] H. Hamaker, *Physica* **1937**, *4*, 1058.

[33] W. Pisula, Z. Tomovic, C. Simpson, M. K. T. Pakula, K. Müllen, *Chem. Mater.* **2005**, *17*, 4296.

[34] T. L. Salter, J. W. Stubbing, L. Brigham, W. A. Brown, *J. Chem. Phys.* **2018**, *149*, 164705.

[35] S. S. Jester, D. Schmitz, F. Eberhagen, S. Höger, *Chem. Commun.* **2011**, *47*, 8838.

[36] E. A. Meyer, R. K. Castellano, F. Diederich, *Angew. Chem. Int. Ed.* **2003**, *42*, 1210.

[37] A. Kiermeier, B. Ernstberger, H. J. Neusser, E. W. Schlag, *J. Phys. Chem.* **1988**, *92*, 3785.

[38] B. Ernstberger, H. Krause, A. Kiermeier, H. J. Neusser, *J. Chem. Phys.* **1990**, *92*, 5285.

[39] A. van der Avoird, R. Podeszwa, K. Szalewicz, C. Leforestier, R. van Harrevelt, P. R. Bunker, M. Schnell, G. von Helden, G. Meijer, *Phys. Chem. Chem. Phys.* **2010**, *12*, 8219.

[40] B. F. Henson, G. V. Hartland, V. A. Venturo, P. M. Felker, *J. Chem. Phys.* **1989**, *91*, 2751.

[41] M. Schnell, U. Erlekam, P. R. Bunker, G. von Helden, J. U. Grabow, G. Meijer, A. van der Avoird, *Angew. Chem. Int. Ed.* **2013**, *52*, 5180.

[42] J. R. Grover, E. A. Walters, E. T. Hui, *J. Phys. Chem.* **1987**, *91*, 3233.

[43] J. M. Steed, T. A. Dixon, W. Klemperer, *J. Chem. Phys.* **1979**, *70*, 4940.

[44] E. Arunan, H. S. Gutowsky, *J. Chem. Phys.* **1993**, *98*, 4294.

[45] R. Podeszwa, R. Bukowski, K. Szalewicz, *J. Phys. Chem. A* **2006**, *110*, 10345.

[46] J. Vollmeyer, F. Eberhagen, S. Höger, S. S. Jester, *Beilstein J. Org. Chem.* **2014**, *10*, 2774.

[47] L. A. Girifalco, M. Hodak, R. S. Lee, *Phys. Rev. B* **2000**, *62*, 13104.